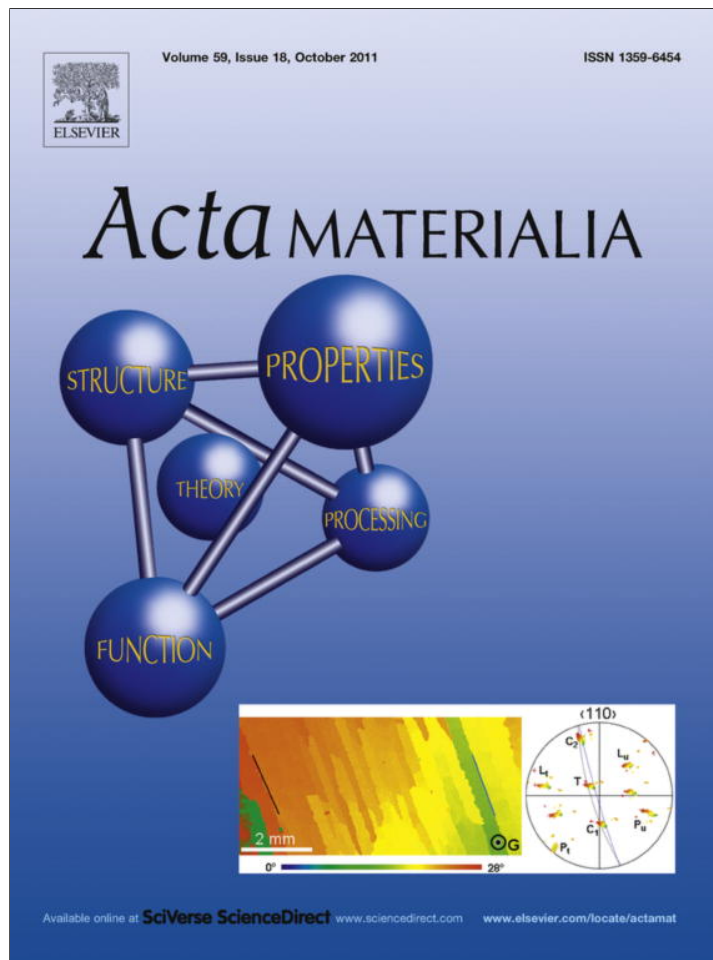


Provided for non-commercial research and education use.
Not for reproduction, distribution or commercial use.



This article appeared in a journal published by Elsevier. The attached copy is furnished to the author for internal non-commercial research and education use, including for instruction at the authors institution and sharing with colleagues.

Other uses, including reproduction and distribution, or selling or licensing copies, or posting to personal, institutional or third party websites are prohibited.

In most cases authors are permitted to post their version of the article (e.g. in Word or Tex form) to their personal website or institutional repository. Authors requiring further information regarding Elsevier's archiving and manuscript policies are encouraged to visit:

<http://www.elsevier.com/copyright>



Thermodynamics and kinetics of nanovoid nucleation inside elastoplastic material

Valery I. Levitas^{a,b,c,*}, Nataliya S. Altukhova^a

^a Iowa State University, Department of Aerospace Engineering, Ames, IA 50011, USA

^b Iowa State University, Department of Mechanical Engineering, Ames, IA 50011, USA

^c Iowa State University, Department of Material Science and Engineering, Ames, IA 50011, USA

Received 21 April 2011; received in revised form 25 July 2011; accepted 27 July 2011

Available online 24 August 2011

Abstract

Continuum thermodynamic and kinetic approaches to nanovoid nucleation as a fracture process inside elastoplastic material are developed. They include solutions to such conceptual problems as determination of the thermodynamic driving force and activation energy, and determination of the kinetic relationship between tensile fracture pressure and temperature. A kinetic pressure–temperature diagram for nanovoid nucleation is determined which, in addition to fracture, includes alternative mechanisms related to phase transformations. Fracture occurs below the kinetic melting temperature, sublimation takes place at high temperature and evaporation occurs in the intermediate range. Sublimation via virtual melting competes with fracture and evaporation.

© 2011 Acta Materialia Inc. Published by Elsevier Ltd. All rights reserved.

Keywords: Nanovoid nucleation; Ductile fracture; Phase transformation; Continuum mechanics model; Nucleation

1. Introduction

Void nucleation, growth and coalescence in elastoplastic (ductile) materials are the main mechanisms of damage, spallation and ductile fracture. Fracture is considered here as breaking atomic bonds and creating new internal surfaces. There is an enormous amount of literature devoted to this topic, including atomistic [1–4] and continuum [5–7] approaches. Our focus here is on development of thermodynamic and kinetic theory for the homogeneous nucleation of a nanovoids in elastoplastic materials. Such nucleation may occur in a tensile stress wave or under static conditions, e.g. near a crack tip. Homogeneous nucleation assumes the lack of preferred nucleation sites (i.e. stress concentrators due to defects or pre-existing surfaces due to grain boundaries and inclusions). This condition is

fulfilled in nanoparticles or in the nanovolume of bulk material, in which the size of the highly stressed region is smaller than the distance between e.g. dislocations, inclusions and grain boundaries. We consider quite high temperatures at which inclusions may dissolve, eliminating the most important nucleation sites for heterogeneous fracture. Note that homogeneous nucleation theory is in good correspondence with experiments for the defect-free case, e.g. for martensitic phase transformations [8] and cavitation [9]. After developing the homogeneous nucleation theory, the effect of defects can be taken into account as the next approximation. We will also not include vacancy-mediated void nucleation and growth due to the Kirkendall effect [10–12], because it is a much slower process than that considered in the current paper. While nucleation theory for voids in liquid (cavitation) has been known for decades [13,14], we are not familiar with a similar theory for elastoplastic solids. The main approaches to void appearance in elastic materials are based on consideration of bifurcation of the solution of a mechanical problem when the energy of the solution with a void is smaller than without one

* Corresponding author at: Iowa State University, Department of Aerospace Engineering, Ames, IA 50011, USA. Tel.: +1 515 294 9691; fax: +1 801 788 0026.

E-mail address: vlevitas@iastate.edu (V.I. Levitas).

[5]. Only in Ref. [7] is the surface energy taken into account. Mechanical solutions for stresses and strains for elastoplastic materials [5,6] do not take into account surface energy and stresses, which makes them inapplicable for the development of the kinetic theory. In Ref. [12], surface stresses were taken into account; however, the results were applied to the void growth due to vacancy diffusion rather than to void nucleation due to fracture. There is also a fundamental problem in the development of thermodynamics for void nucleation in elastoplastic material. For void nucleation in an elastic solid (e.g. soft polymeric and rubber-like materials), a difference in the Gibbs potential of the system before and after void nucleation is the driving force for fracture (i.e. it is dissipation due to fracture) [15,16] and the activation energy is equal to the Gibbs energy of a critical nucleus. Since void nucleation in a crystalline solid is accompanied by large plastic deformation – i.e. it involves irreversibilities (dissipation) – the traditional approach is not applicable, and one needs to develop concepts for the thermodynamic driving force and activation energy for void nucleation. For irreversible processes, it is not sufficient to compare energy of the final and initial stages; rather, the entire process of void formation should be taken into account. This problem is similar to that for the theory of phase transformation in elastoplastic materials [17–21]. One of the key points here is to define the thermomechanical process that leads to void formation and to separate dissipation due to fracture and plastic dissipation. In an existing thermodynamic attempt [18–20], fracture is defined as a second-order phase transition in some finite region in which tensile and shear elastic moduli, and all material parameters, change from initial values to zero. As a result, the driving force in Ref. [19,20] depends on the thermal part of free energy, which is contradictory. In the current paper, we define a thermomechanical process that is free from this contradiction, derive the expressions for the driving force and activation energy for void nucleation, calculate them for a spherical void based on our generalization of the large-strain solution with allowance for surface energy [21], and determine the kinetic relationship between tensile pressure and temperature for the appearance of the critical nanovoid. An important point is that all the results are expressed in terms of parameters at the void interface, which makes them independent of the material's constitutive behavior. In particular, the universal driving force for the void nucleation (i.e. the dissipation due to fracture only) for any material is the difference between work produced by external traction acting on the void surface and work produced by the Laplacian pressure $2\gamma/R$, where γ is the surface energy and $1/R$ is the mean curvature. However, the external traction acting on the void surface and its work are determined by solution of the boundary value problem and depend on the constitutive equations. In addition to these main results, similar kinetic relationships are found for void nucleation based on alternative phase-transformation-related mechanisms – namely, due to direct sublimation, sublimation via virtual

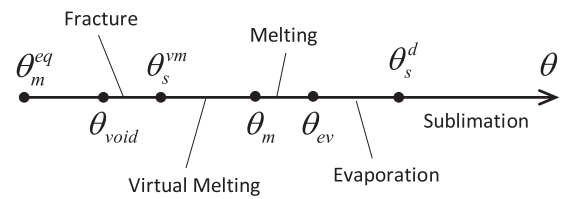


Fig. 1. Schematics for characteristic temperatures under tensile pressure. θ_m^{eq} is the thermodynamic equilibrium melting temperature; $\theta_m > \theta_m^{eq}$ is the kinetic melting temperature, above which a critical melt nucleus appears and causes complete melting of the solid; $\theta_{ev} \geq \theta_m$ is the melt evaporation temperature; sublimation temperature is designated θ_s^d ; the temperature for sublimation via virtual melting θ_s^{vm} is located between θ_m^{eq} and θ_m ; and θ_{void} is the temperature for void nucleation due to fracture. All the processes shown in the schematics occur above the corresponding characteristic temperatures provided that the processes shown at lower temperature did not occur.

melting and evaporation of stable liquid that nucleates due to melting – that were obtained using our approaches from Ref. [21,22] (Fig. 1). This allowed us to find regions where each of the above mechanisms is the kinetically favorable one, which completely changes the results presented in Ref. [21,22]. Sublimation is considered as an appearance of the gaseous critical nucleus in solid due to solid–gas transformation, i.e. transformation of a critical volume of solid to gas. Above the kinetic melting temperature θ_m (the temperature above which a critical melt nucleus appears and causes complete melting of the solid), we consider complete melting followed by transformation of a critical volume of liquid into gas (evaporation). In the temperature range below θ_m but above the equilibrium melting temperature θ_m^{eq} , a subcritical liquid drop may appear and transform to the critical vapor nucleus; we called this process “sublimation via virtual melting” [22]. In more detail, while in this temperature range, nucleation of the supercritical liquid nucleus is impossible, but numerous subcritical liquid nuclei exist inside the solid. As soon as the kinetic criterion for vaporization of some of them is fulfilled, subcritical liquid nuclei immediately transform into critical gas nuclei. Thus, such a melt represents an intermediate (transitional) state between solid and vapor; as soon as subcritical melt droplets nucleate, they immediately become unstable with respect to vapor. That is why such a melt is called virtual melt, similar to the virtual melt in crystal–crystal [23,24] and crystal–amorphous [25] phase transformations, which we predicted earlier.

It was found that fracture occurs below the kinetic melting temperature and under large pressure; sublimation takes place at very high temperature and small pressure; and evaporation occurs for the intermediate range. Since the curve for sublimation via virtual melting is very close to the fracture curve (for low surface energy and above thermodynamic melting temperature) or the sublimation curve (for high surface energy and above kinetic melting temperature), sublimation via virtual melting competes with these processes.

Vectors and tensors are denoted in boldface type; $\mathbf{p} \cdot \mathbf{v}$ is the scalar product of vectors \mathbf{p} and \mathbf{v} ; $\mathbf{A}:\mathbf{B}$ designates

contractions of tensors \mathbf{A} and \mathbf{B} over two indices. We will ignore the difference between the surface energy γ and tension (stresses) (see the review by Fischer et al. [26]).

2. Thermodynamic driving force for fracture

Let us consider the elastoplastic body of mass m and volume V in the current state bounded by the external surface S in the current state (Fig. 2).

Let the traction vector \mathbf{p} be applied on part of the external surface S_p and the displacement vector \mathbf{u} be prescribed on another part S_u , $S = S_p + S_u$; mixed boundary conditions can be considered similar. We define the void nucleation due to fracture as a thermomechanical process of growth of a cavity inside a solid from zero to some critical size due to bond breaking. We start with the expression for the dissipation rate in a volume V and a growing surface Σ of an internal cavity,

$$D = \int_S \mathbf{p} \cdot \mathbf{v} dS - \dot{\Psi} - \dot{\Gamma} \quad (1)$$

where $\Psi = \int_m \psi dm$ are the total and specific Helmholtz free energy, $\Gamma = \int_\Sigma \gamma d\Sigma$ and γ are the total and specific (per unit current area Σ) surface energy of a void, and \mathbf{v} is the particle velocity. The total dissipation rate consists of contributions due to fracture and plastic flow. To find the driving force for fracture, the dissipation rate due to fracture only should be defined:

$$D_f = D - D_p \quad (2)$$

where

$$D_p = \int_m \rho^{-1} \mathbf{T} : \mathbf{d}_p dm \quad (3)$$

is the plastic dissipation rate, ρ is the mass density in the deformed state, \mathbf{d}_p is the plastic deformation rate and \mathbf{T} is the true Cauchy stress tensor. This is similar to the approach developed for phase transformations in plastic materials [17–22,27]: the driving force for phase transformation is the dissipation rate due to phase transformation only, which is the difference between the total dissipation

rate and the plastic dissipation rate. To make our approach consistent with the approach for fracture in elastic materials (see below) and phase transformations in plastic materials, the dissipation rate due to fracture only should be averaged over the nucleation process or time t_n

$$\overline{D}_f := \frac{1}{t_n} \int_0^{t_n} D_f dt = \frac{X_f}{t_n} = X_f \dot{\lambda} \quad (4)$$

where

$$X_f := \int_0^{t_n} \int_S \mathbf{p} \cdot \mathbf{v} dS dt - \Delta\Psi - \int_0^{t_n} D_p dt - \Delta\Gamma \quad (5)$$

$$\text{and } \dot{\lambda} := \frac{1}{t_n}$$

are the dissipative (driving) forces for fracture and rate, respectively, and $\Delta = a_2 - a_1$ means an increment of a function between state 1 before and state 2 after nucleation. Since the void starts to grow from zero size, $\Gamma_1 = 0$ and $\Delta\Gamma = \Gamma$. To make the mechanical interpretation clearer, we can show that the surface energy can be considered as the work produced by the Laplacian pressure. Indeed, application of the transport theorem for moving surfaces (see e.g. [16,28]) for $\gamma = const$ gives

$$\dot{\Gamma} = \frac{d}{dt} \int_\Sigma \gamma d\Sigma = \int_\Sigma \frac{2\gamma}{R} v_n d\Sigma$$

$$\text{and } \Gamma = \int_0^{t_n} \dot{\Gamma} dt = \int_0^{u_{n2}} \int_\Sigma \frac{2\gamma}{R} du_n d\Sigma \quad (6)$$

where v_n and u_n are the normal components of the velocity and displacement of the void surface Σ , respectively, $1/R$ is the mean curvature and $2\gamma/R$ is the Laplacian pressure (i.e. jump in normal component of stresses across an interface). This is why for the mechanics problem we included the Laplacian pressure at the void surface along the normal to Σ .

The above expression for the driving force for fracture X_f can be simplified. Since X_f is the dissipation increment due to fracture only, integrals in Eq. (5) (excluding the integral over Σ) can be evaluated over an arbitrary material volume with a fixed mass and bounding surface S' that includes the void (nucleus) – i.e. the driving force for

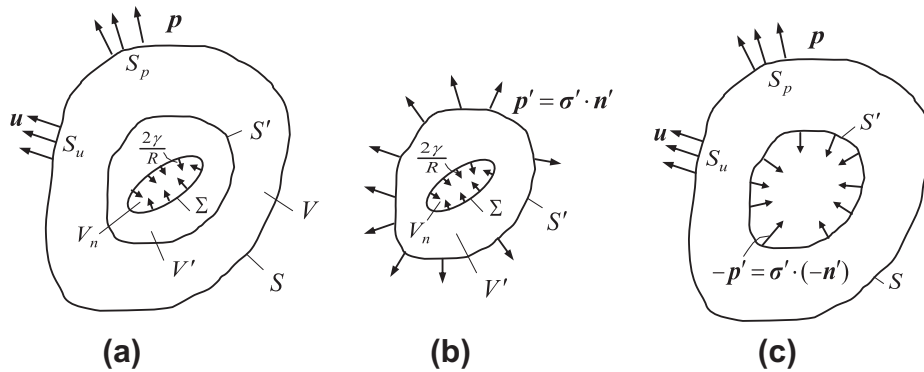


Fig. 2. (a) Scheme of the elastoplastic body under prescribed tractions \mathbf{p} and displacements \mathbf{u} at parts S_p and S_u of the external surface, with the nucleating void of the volume V_n bounded by the surface Σ . Laplacian pressure $2\gamma/R$ is directed along the normal to the void surface. (b) The void nucleation criterion can also be expressed for the arbitrary volume V' inside the surface S' containing the void. (c) Remaining volume $V - V'$ with the applied loading.

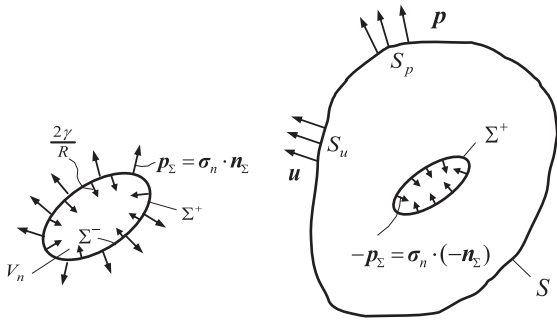


Fig. 3. The same as in Fig. 2b and c, for the case when surface S' is chosen as the surface Σ^+ that is infinitesimally close to the void surface Σ from the solid side. Surface Σ^- is infinitesimally close to the void surface Σ from the void side.

fracture is the volume-independent integral. Indeed, in the remaining volume, $X_f = 0$ because of lack of fracture. Fig. 2b and c shows corresponding schematics and tractions applied to different surfaces. Note that, while tractions and displacements at the external surface S are given, tractions \mathbf{p}' at the arbitrary chosen surface S' are to be found from the solution of the elastoplastic boundary-value problem.

In particular, the material volume and mass may coincide with the final volume V_{n2} and mass m_2 of the critical nucleus. The mass of the void is zero before nucleation (since no void exists) and after; $\mathbf{d}_p = 0$ because of lack of plastic deformation inside the void; before nucleation, $\Gamma_1 = 0$; and $\mathbf{u}_1 = 0$, where \mathbf{u} is the particle displacement vector.

Thus, surface S' in the given case can be inside the solid infinitesimally close to the void surface Σ and will be designated as Σ^+ (Fig. 3). In this case, one has

$$X_f := \int_0^{u_2} \int_{\Sigma^+} \mathbf{p}_\Sigma \cdot d\mathbf{u}_\Sigma d\Sigma^+ - \Gamma \quad (7)$$

where $\mathbf{p}_\Sigma = \boldsymbol{\sigma}_\Sigma \cdot \mathbf{n}_\Sigma$ and $\boldsymbol{\sigma}_\Sigma$ are the traction and stress tensor at Σ^+ . Note that, while inside the nucleating void all stresses are zero, the surface traction infinitesimally close to the void surface Σ (that will be designated as Σ^- from the side of the void) is equal to the Laplacian pressure $2\gamma/R$ along the internal normal to the Σ .

Thus, the expression for the driving force for void nucleation, Eq. (7), is completely localized at the void growing surface and does not contain a term with plastic dissipation. This is because the plastic zone is located outside the fracture zone, and thus integral Eq. (5) is identically zero in the plastic zone (because there is no fracture in it). This is similar to the consideration of phase transformation in elastoplastic materials [17–22,27] when the driving force is calculated as the integral over the nucleus only; if there is no plastic strain inside the nucleus (e.g. like for sublimation or sublimation via the virtual melting [21,22]), then plastic dissipation disappears from the final expression for the driving force. Plastic deformation, however, does affect the void nucleation because it determines the traction \mathbf{p}_Σ at the void surface in the expression for X_f .

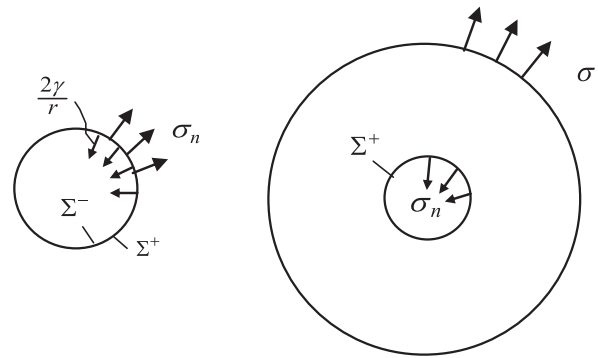


Fig. 4. The same as in Fig. 3 but for a spherical void in a large sphere under normal external stress σ_n . Normal stress σ_n acts in the solid at the surface Σ^+ and the Laplacian pressure $2\gamma/r$ is applied at the surface Σ^- . Both these surfaces are infinitesimally close to the void surface Σ from the side of the solid and void, respectively.

Substituting expression (6) for Γ in Eq. (7) results in

$$X_f = \int_0^{u_2} \int_{\Sigma} \mathbf{p}_\Sigma \cdot d\mathbf{u}_\Sigma d\Sigma - \int_0^{u_2} \int_{\Sigma} \frac{2\gamma}{R} du_n d\Sigma \quad (8)$$

where we took into account that the surfaces Σ , Σ^+ and Σ^- are infinitesimally close. Thus, the driving force for the void nucleation (which is the dissipation due to fracture only) is the difference between work produced by external traction acting on the void surface \mathbf{p}_Σ and work produced by the Laplacian pressure $\frac{2\gamma}{R}$. For a spherical void of a radius r under axisymmetric loading, $\mathbf{p}_\Sigma \cdot d\mathbf{u}_\Sigma = \sigma_n du_n$, $du_n = dr$, where σ_n is the normal tensile stress in the solid at the void surface Σ^+ (Fig. 4).

Then Eq. (8) can be simplified to

$$X_f = \int_0^{r_c} \int_{\Sigma} \left(\sigma_n - \frac{2\gamma}{r} \right) dr d\Sigma \quad (9)$$

where r_c is the radius of the critical nucleus. A geometric interpretation of Eq. (9) is given in Fig. 5: the driving force X_f is the area enclosed between the curves σ_n and $\frac{2\gamma}{r}$; it is negative, and will determine the energy necessary for void nucleation, which comes from thermal fluctuations (see Section 4).

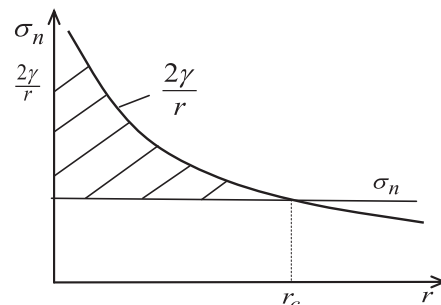


Fig. 5. Normal stress σ_n applied to the void surface from the side of the solid and the Laplacian pressure vs. void radius for a spherically symmetric problem. Mechanical equilibrium conditions at the interface are satisfied for the critical nucleus only. For a subcritical nucleus, the applied stress σ_n is smaller than the Laplacian pressure and thermal fluctuations need to supply the activation energy equal to the dashed area. For supercritical nucleus, the applied stress σ_n is larger than the Laplacian pressure; such a nucleus is mechanically unstable and will grow.

Note that the definitions of the driving force in Eqs. (5)–(8) are independent of the type of material (e.g. elastoplastic solid, viscoelastic or viscoplastic solid, or liquid) because we derived them without specifying the constitutive equations and the plastic dissipation rate. In fact, Eqs. (7) and (8) do not contain a plastic dissipation rate. Constitutive equations come into play for solution of the boundary-value problem to connect traction on the external surface and on the surface of the void.

3. Fracture in elastic material

During the nucleation process, let the traction vector $\mathbf{p} = \mathbf{const} = \mathbf{p}_0$ be fixed on part of the external surface S_p and the displacement vector $\mathbf{u} = \mathbf{const}$ on another part S_u , $S = S_p + S_u$. Then,

$$\int_{\mathbf{u}_1}^{\mathbf{u}_2} \int_{S_p} \mathbf{p} \cdot d\mathbf{u} dS = \int_{S_p} \mathbf{p}_0 \cdot (\mathbf{u}_2 - \mathbf{u}_1) dS_p \quad (10)$$

For elastic materials, $\mathbf{d}_p = 0$. Introducing the Gibbs potential,

$$G := \Psi + \Gamma - \int_{S_p} \mathbf{p} \cdot \mathbf{u} dS_p \quad (11)$$

we obtain from Eq. (5) that

$$X_f = G_1 - G_2 = -\Delta G \quad (12)$$

i.e. that the driving force for fracture is the minus change in the Gibbs potential, as required. This demonstrates the consistency of our general approach with results for elastic materials and justifies averaging over the nucleation process. Our approach to the driving force, particularly the exclusion of plastic dissipation, is also consistent with the approach for phase transformation in plastic materials [17–19,21].

An activation energy for a spherical void in elastic material is determined by

$$Q = \max_r \Delta G$$

i.e. the critical nucleus corresponds to the maximum of the energy of the nucleus with respect to the void radius r , and Q is equal to the energy of the critical nucleus. Similarly, for elastoplastic material, the activation energy is defined as

$$Q = \max_r (-X_f) = -\min_r X_f \quad (13)$$

i.e. the critical nucleus corresponds to the minimum of the driving force for fracture vs. the void radius, and Q is equal to the magnitude of the driving force for the critical nucleus.

4. Critical nucleus in elastoplastic material

For the arbitrary void shape in elastoplastic material,

$$Q = \max_a \min_{shape} \min_{path} (-X_f) \quad (14)$$

where a is the characteristic size, and minimization is performed with respect to shape of void and path along

which this shape was changed, since the behavior of the plastic material is path-dependent.

Since the critical nucleus should be in metastable thermodynamic and mechanical equilibrium, the equilibrium condition at the interface of the critical void is (Fig. 5)

$$\sigma_n = \frac{2\gamma}{R_c} \quad (15)$$

where $\sigma_n > 0$ is the normal tensile stress in the solid at the interface (Fig. 4). The tensile stress σ_n that can be carried by an elastoplastic material is finite [29,5]. That is why Eq. (15) cannot be satisfied for the curvatures above some critical value (Fig. 5), which means that it can be satisfied for the critical nucleus only. For the size of a cavity larger than the critical nucleus, $\sigma_n > 2\gamma/R$ and the void will grow under constant external load because σ_n is practically constant during small changes in the void size (see below). Thus, Eq. (15) gives us an alternative definition of the critical nucleus to Eq. (14). Note that, according to Eq. (8), the activation energy represents the difference between the work of the normal traction \mathbf{p}_Σ and the Laplacian pressure that should be overcome by thermal activation (Fig. 5). For an arbitrary void, it is reasonable to assume that, while equilibrium Eq. (15) is not valid, traction $\mathbf{p}_\Sigma = \sigma_\Sigma \cdot \mathbf{n}_\Sigma$ for subcritical nucleus is still directed along the normal \mathbf{n}_Σ to the void surface Σ^+ .

The Arrhenius-type relationship for time of appearance of the critical nucleus is

$$t_n = t_0 \exp\left(\frac{Q}{k\theta}\right) \quad (16)$$

where k is the Boltzmann constant and t_0 is the inverse frequency factor. The usual way to determine a kinetic relationship between parameters for the critical nucleus (e.g. pressure and temperature) is to use the kinetic nucleation criterion

$$Q = \beta k\theta, \quad (17)$$

with $\beta = 40 \div 80$, which is determined from the condition that, for larger Q , the nucleation time exceeds any realistic time of observation for any t_0 [30,31].

5. Spherical void

Let us apply the developed theory to a spherical void nucleation in an infinite elastoplastic sphere under external tensile pressure σ (Fig. 4).

The solution to the large-strain ideal-plastic problem on expansion of a spherical hole from zero size with ignored elastic strain is [29,21]

$$\sigma_n = \sigma - \sigma_c; \quad \sigma_c := \frac{2}{3} \sigma_y \left(1 + \ln\left(\frac{2\mu\alpha}{3\sigma_y}\right)\right). \quad (18)$$

Here, the von Mises yield condition was used; σ_c is the cavitation pressure, which is the possible maximum value of tensile pressure that a solid can sustain if the surface energy is ignored; $\alpha = \frac{1+v}{1-v}$, v is Poisson's ratio; μ is the shear modulus; and σ_y is the yield strength. Then, the work

$$\int_{u_1}^{u_2} \int_{\Sigma^+} \mathbf{p}_{\Sigma} \cdot d\mathbf{u}_{\Sigma} d\Sigma^+ = \sigma_n V_n \quad (19)$$

where V_n is the volume of the void. Also,

$$X_f = \sigma_n \frac{4}{3} \pi r_c^3 - \gamma 4\pi r_c^2 \quad (20)$$

where $r_c = R_c$ is the critical radius of the void. Minimization of X_f with respect to r_c leads to equilibrium Eq. (15) for the critical nucleus. Surprisingly, Eq. (20) looks exactly like the one for cavitation in liquid [13,14] if the tensile pressure in the liquid σ is substituted by the constant normal stress at the void surface σ_n (Eq. (18)). It also looks like the driving force for phase transformation if σ_n in Eq. (20) is substituted by the change in the specific Gibbs energy. Then, from Eqs. (15) and (20) and $Q = -X_f$, one obtains for the critical void radius and activation energy

$$r_c = \frac{2\gamma}{\sigma_n}; \quad Q = \frac{16\pi\gamma^3}{3\sigma_n^2} \quad (21)$$

Substituting Q in the kinetic nucleation criterion Eq. (17) and combining it with Eq. (18) for σ_n , we obtain the explicit relationship between tensile pressure for nanovoid nucleation σ and temperature:

$$\sigma_n = \sigma - \sigma_c = \left(\frac{16\pi\gamma^3}{3\beta k\theta} \right)^{1/2} \quad (22)$$

where the mechanical properties are a function of temperature. For void nucleation in liquid (cavitation), $\sigma_c = 0$. Thus, the kinetic $\sigma - \theta$ void nucleation curve for an elastoplastic solid can be obtained from the cavitation curve for liquid by shifting it to the right by σ_c . In fact, Eq. (22) for σ_n is valid for any type of material, e.g. for a viscous (creeping) or viscoplastic solid or liquid; specific constitutive properties contribute to the expression for σ_n vs. applied stress σ .

The temperature dependence of σ_y is scaled with the temperature dependence of μ , i.e. μ/σ_y , as well as Poisson's ratio, and consequently α , are weakly temperature dependent. Below, we will use the simple approximation

$$\sigma_y = \sigma_y^r + (\sigma_y^m - \sigma_y^r) \frac{\theta - \theta_r}{\theta_m - \theta_r} \quad \text{for } \theta < \theta_m \quad (23)$$

and

$$\sigma_y = \bar{\sigma}_y \quad \text{for } \theta > \theta_m \quad (24)$$

where θ_m and θ_r are the melting and room temperatures, respectively, and σ_y^m and σ_y^r are the yield strengths at these temperatures. For slow heating and loading, $\bar{\sigma}_y = 0$. However, we will focus on very fast heating and loading, when material still remains solid above the melting temperature beyond the melt nucleation time; we will use $\bar{\sigma}_y = \sigma_y^m$.

Taking into account indeterminacy in melting temperature at very high heating rates and in $\bar{\sigma}_y$, the pressure dependence of the melting temperature in the equation for σ_y can be ignored. The results can be expressed in dimensionless variables σ/σ_c^m and θ/θ^* and will depend up

the dimensionless parameters σ_y^m/σ_y^r , θ_m/θ_r and $\left(\frac{16\pi\gamma^3}{3\beta k\theta^* \sigma_c^m} \right)^{1/2}$; here, $\sigma_c^m := \sigma_c(\theta_m)$ is the cavitation pressure at the melting temperature and θ^* is any chosen characteristic temperature (i.e. θ_m or θ_r). Having in mind that we would like to compare results on void nucleation with our previous results on sublimation and sublimation via virtual melting [21,22], we chose the same data as in Ref. [21,22] (which are close to the data for energetic crystal HMX, if known):

$$\sigma_y^m = 2.6 \text{ MPa}, \quad \sigma_y^r/\sigma_y^m = 14.23, \quad \theta_r = 300 \text{ K}, \quad \nu = 0.3, \\ \theta_m/\theta_r = 1.833, \quad \mu/\sigma_y = 2623, \quad \text{and } \beta = 80$$

This results, in particular, in $\sigma_c^m/\sigma_y^m = 6.07$ and $\sigma_c^m = 15.78 \text{ MPa}$. We also chose, as in Refs. [21,22], $\theta^* = 784.12 \text{ K}$ (instead of θ_m or θ_r , which we would have chosen were we considering fracture only), which is the sublimation temperature for $\sigma = 0$, and ignored the surface energy.

The results for void nucleation due to fracture (Eq. (22)) are presented in Fig. 6 for several values of surface energy and yield strength. The lowest curve for each surface energy corresponds to $\sigma_y^r = \sigma_y^m = 0$, i.e. to cavitation in liquid.

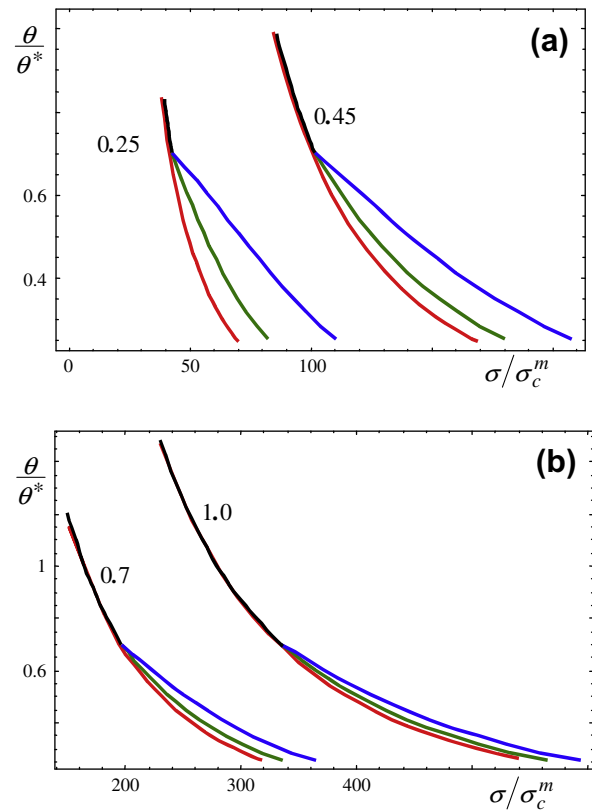


Fig. 6. Calculated temperature–tensile pressure curves for appearance of a spherical void within elastoplastic solid due to fracture for several values of surface energy (shown near curves in J m^{-2}), $\sigma_y^r/\sigma_y^m = 56.92$ (upper curve) and $\sigma_y^r/\sigma_y^m = 14.23$ (middle curve). The lowest curve corresponds to $\sigma_y^r = \sigma_y^m = 0$ (still keeping $\sigma_c^m = 15.78 \text{ MPa}$ for normalization of σ), i.e. to cavitation in liquid.

As was recently suggested in Ref. [21,22], void nucleation may occur due to completely different, phase-transformation-related mechanisms, namely due to direct sublimation, sublimation via virtual melting and evaporation of stable liquid that nucleates due to melting. To obtain a complete kinetic diagram for void nucleation due to all the currently studied processes (Figs. 7 and 8), the results for fracture are supplemented by the results for phase-transformation-related mechanisms, obtained using our approaches from [21,22].

Sublimation is considered to be the transformation of a critical volume of solid to gas. Above the kinetic melting temperature θ_m (the temperature above which a critical melt nucleus appears and causes complete melting), we consider complete melting and transformation of a critical volume of liquid into gas (evaporation). Below θ_m but above the equilibrium melting temperature θ_m^{eq} , a subcritical liquid drop may appear and transform into the critical vapor nucleus; we call this process sublimation via virtual melting [22]. In addition to [21,22], we take into account the elastic deformation regime for small σ and temperature dependence of the yield strength. Also, the curve for “evaporation” in Fig. 8 differs significantly from that in Ref. [22] because in Ref. [22] “evaporation” was considered as

sublimation of solid HMX with zero yield strength (to demonstrate the effect of the yield strength), and here we consider the actual evaporation of the HMX melt. This changes the regions of kinetic advantage of sublimation and evaporation.

First, we compare results for fracture and sublimation only. In Fig. 7, for each value of the surface energy there is the critical temperature, below which fracture is kinetically more favorable and above which sublimation occurs. While the critical temperature is close to the temperature at which sublimation occurs at $\sigma = 0$, quite a large tensile pressure should be applied to cause fracture. If melting or virtual melting cannot occur in the pressure and temperature ranges under consideration, these are the only two possible scenarios for a void nucleation.

The complete kinetic diagram (Fig. 8) is completely different from that in Ref. [22]. The lowest lines for each pressure σ (and lines that are very close to the lowest)

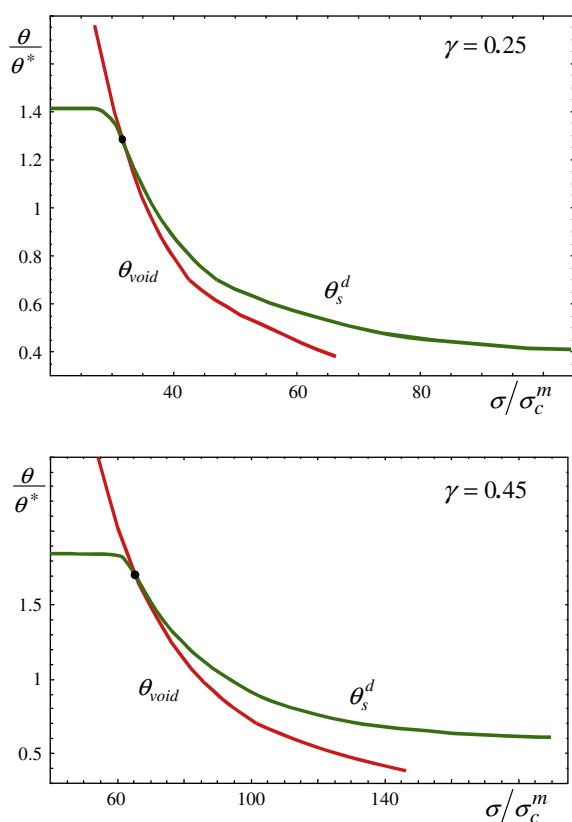


Fig. 7. Calculated temperature–tensile pressure curves for the appearance of a spherical void within an elastoplastic solid due to sublimation θ_s^d (green line) and fracture θ_{void} (red line) for the two values of solid–gas surface energy shown in the right corner in J m^{-2} . (For interpretation of the references to color in this figure legend, the reader is referred to the web version of this article.)

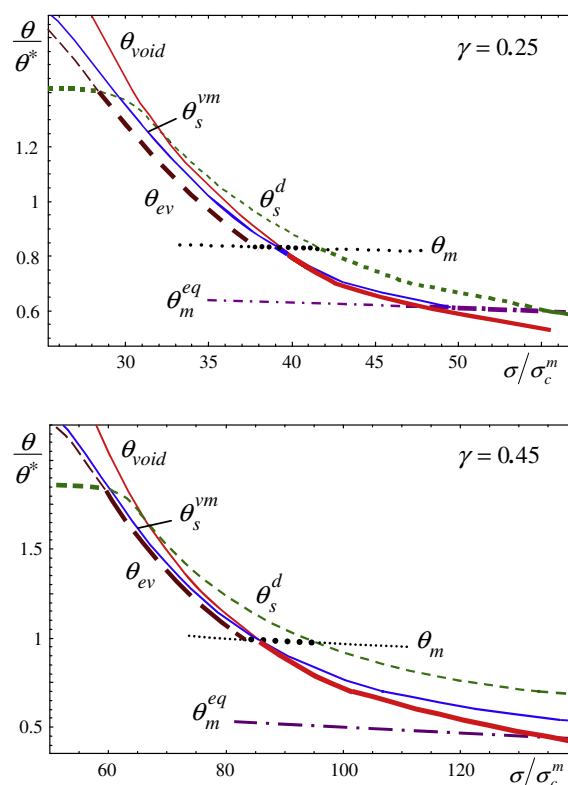


Fig. 8. Kinetic temperature–tensile pressure criteria for the appearance of a spherical void due to fracture, sublimation, sublimation via virtual melting and evaporation of a liquid drop within an elastoplastic solid for two values of surface energy (shown in the right corner in J m^{-2}). The following designations of the curves are used: for fracture, θ_{void} (red solid line); for direct sublimation, θ_s^d (green dashed line); for sublimation via virtual melting, θ_s^{vm} (blue solid line); for melting, θ_m (black dotted line); for evaporation of melt, θ_{ev} (brown dash-style line); and for thermodynamic equilibrium melting, θ_m^{eq} (magenta dashed-dotted line). The bold parts of the curves correspond to the lowest temperature for a given tensile pressure at which a critical void can appear. With increasing tensile pressure, they correspond first to direct sublimation, then to evaporation of liquid, sublimation via virtual melting (for $\gamma = 0.25 \text{ J m}^{-2}$ only) and fracture. (For interpretation of the references to color in this figure legend, the reader is referred to the web version of this article.)

correspond to physically occurring processes because they are kinetically favorable. Thus, in the most important region below the kinetic melting temperature (which reduces with growing σ), fracture occurs. In Ref. [22], in contrast, sublimation occurred below θ_m^{eq} , and sublimation via virtual melting took place below θ_m and above θ_m^{eq} . For small stresses and high temperatures, direct sublimation is significantly kinetically more favorable than all other scenarios; in this region, the sublimation temperature is practically independent of tensile pressure. In Ref. [22], by contrast, “evaporation” occurred in this region. At larger stresses and above the kinetic melting temperature θ_m , the evaporation curve is the lowest one, while in Ref. [22] the lowest curve was for sublimation via virtual melting with some “evaporation” region, reducing with growing surface energy. Below θ_m but above the equilibrium melting temperature θ_m^{eq} , a subcritical liquid drop may appear (virtual melting) and transform into the critical vapor nucleus. This process competes kinetically with fracture. While for $\gamma = 0.45 \text{ J m}^{-2}$ the fracture curve is below the virtual melting curve for all temperatures in this range, for $\gamma = 0.25 \text{ J m}^{-2}$ there is a small temperature range just below θ_m for which sublimation via virtual melting is kinetically more favorable. With the reduction of surface energy, this region expands. Since for any surface energy there is a temperature range for which both curves are quite close, both void nucleation mechanisms may occur simultaneously. Above θ_m for large surface energy, sublimation via virtual melting competes with evaporation.

6. Concluding remarks

In the paper, continuum thermodynamic and kinetic approaches to nanovoid nucleation as a fracture process inside an elastoplastic material are developed. The conceptual problems of determination of the thermodynamic driving force and activation energy, and the determination of the kinetic relationship between the tensile fracture pressure and temperature, are solved. Our general Eqs. (4)–(15) have universal character, i.e. they are independent of the constitutive equations and can be applied for any dissipative material. Eq. (5) is consistent with the approach for fracture in elastic materials. Our approach to the driving force, particularly exclusion of plastic dissipation, is also consistent with the approach for phase transformation in plastic materials [17–19,21]. A kinetic tensile pressure–temperature diagram for the critical nanovoid nucleation due to fracture inside a plastic material is determined. Similar kinetic relationships are found for void nucleation based on alternative competing mechanisms, namely due to direct sublimation, sublimation via virtual melting and evaporation of stable liquid that nucleates due to melting. The regions where each of the above mechanisms is kinetically favorable are found. They are completely different from those in Ref. [22] because of adding fracture and evaporation.

It is clear that utilizing continuum concepts at the nanoscale can be questioned both for elastic and elasto-

plastic materials. However, they are routinely used in classical nucleation theory, despite the fact that the size of the critical nucleus can be from one to several interatomic distances. Our objective was to conceptually advance the nucleation theory for the case with inelastic deformation and thermodynamic irreversibility in the simplest possible way, as we did for sublimation and sublimation via virtual melting [21,22]. Since the results of application of classical nucleation theory are in good correspondence with experiments involving the defect-free case (in particular, for cavitation [9] and martensitic phase transformations [8]), and because they are widely used for analysis of nucleation at the nanoscale (e.g. for melting [32]), we assume that our generalization of the nucleation theory will also correspond well with future experiments. There are many other cases for which continuum thermodynamic and mechanics operate adequately below their expected limit of small-size applicability, e.g. for the description of deformation of a single-wall carbon nanotube or phase interface a few interatomic distances thick in the phase field approach [33].

The method to check our predictions is similar to that described in Ref. [21,22]. A similar approach can be applied to the thermodynamics and kinetics of crack propagation in an inelastic material [19,20,34]. As the next step, size- and strain-dependence of the surface energy, as well as the presence of defects (e.g. grain boundaries), have to be taken into account. Also, diffusion-induced void nucleation due to the Kirkendall effect [10,11] will be studied, and its competition with the above processes will be analyzed.

Acknowledgements

The support of the National Science Foundation (Grant CBET-0755236, managed by Drs. Phillip Westmoreland and Arvind Atreya, and Grant CMMI-0969143, managed by Dr. Glaucio Paulino), the Army Research Office (Grant W911NF-09-1-0001, managed by Drs. David Stepp and Suveen Mathaudhu), Iowa State University and Texas Tech University are gratefully acknowledged.

References

- [1] Makino M, Tsuji T, Noda N. *Comput Mech* 2000;26(3):281–7.
- [2] Marian J, Knap J, Ortiz M. *Phys Rev Lett* 2004;93(16):165503.
- [3] Dongare AM, Rajendran AM, LaMattina B, Zikry MA, Brenner DW. *Phys Rev B* 2009;80(10):104108.
- [4] Bringa EM, Traiviratana S, Meyers MA. *Acta Mater* 2010;58(13):4458–77.
- [5] Hou HS, Abeyaratne R. *J Mech Phys Solids* 1992;40(3):571–92.
- [6] Wright T, Ramesh K. *J Mech Phys Solids* 2008;56(2):336–59.
- [7] Biwa S. *Int J Non-Linear Mech* 2006;41(9):1084–94.
- [8] Lin M, Olson G, Cohen M. *Acta Metall Mater* 1993;41:253–63.
- [9] Zheng Q, Durben D, Wolf G, Angell C. *Science* 1991;254:829–32.
- [10] Yin Y, Rioux RM, Erdonmez CK, Hughes S, Somorjai GA, Alivisatos AP. *Science* 2004;304:711–4.
- [11] Fischer F, Svoboda J. *Scripta Mater* 2008;58:93–5.
- [12] Fischer F, Antretter T. *Int J Plast* 2009;25:1819–32.
- [13] Zeldovitch YB. *Acta Phys USSR* 1943;18:1–22.

- [14] Fisher JC. *J Appl Phys* 1948;19:1062–7.
- [15] Grinfeld MA. *Doklady Akad Nauk SSSR* 1980;251:10–4.
- [16] Grinfeld MA. *Thermodynamic methods in the theory of heterogeneous systems*. Longman; 1991.
- [17] Levitas V. *Int J Solids Struct* 1998;35:889–940.
- [18] Levitas VI. *Int J Plast* 2000;16:805–49, 851–2.
- [19] Levitas V. *Int J Plast* 2000;16:851–92.
- [20] Idesman AV, Levitas VI, Stein E. *Int J Plast* 2000;16(7–8):893–949.
- [21] Levitas VI, Altukhova N. *Phys Rev Lett* 2008;101(14):145703.
- [22] Levitas VI, Altukhova N. *Phys Rev B* 2009;79(21):212101.
- [23] Levitas V, Henson B, Smilowitz L, Asay B. *Phys Rev Lett* 2004;92:235702.
- [24] Levitas V, Henson B, Smilowitz L, Asay B. *J Phys Chem B* 2006;110(20):10105–19.
- [25] Levitas V. *Phys Rev Lett* 2005;95(7):075701.
- [26] Fischer F, Waitz T, Vollath D, Simha N. *Prog Mater Sci* 2008;53:481527.
- [27] Levitas V. *Int J Plast* 2002;18:1499–525.
- [28] Cermelli P, Fried E, Gurtin M. *J Fluid Mech* 2005;544:339–51.
- [29] Hill R. *The mathematical theory of plasticity*. Oxford: Clarendon press; 1950.
- [30] Porter D, Easterling K. *Phase transformation in metals and alloys*. New York: Van Nostrand Reinhold; 1992.
- [31] Levitas V. *Continuum mechanical fundamentals of mechanochemistry*. In: Gogotsi Y, Domnich V, editors. *High pressure surface science and engineering*. Bristol: Inst. Physics; 2004. p. 159–292.
- [32] Lu K, Li Y. *Phys Rev Lett* 1998;80(20):4474–7.
- [33] Levitas V, Samani K. *Nat Commun* 2011;2:284.
- [34] Simha N, Fischer F, Shan G, Chen C, Kolednik O. *J Mech Phys Solids* 2008;56:2876–95.